# Radiative Heat Feedback in Aluminized Solid Propellant Combustion

M. Quinn Brewster* and David L. Parry†
*University of Illinois, Urbana, Illinois*

**A one-dimensional model has been developed to describe the combustion, flow, and radiant transport processes by aluminum and alumina particles near the surface of a burning aluminized composite solid propellant. The equations of mass, momentum, and energy have been solved to obtain the species concentration, velocity, and temperature profiles near the propellant surface. The decoupled radiative transfer equation has also been solved using the two-flux model to obtain the radiant flux profiles and the radiative heat feedback to the propellant surface. The results of the model indicate that the radiant heat feedback to the surface of a typical aluminized composite propellant would be 300–400 W/cm² or about 20% of the total energy flux required to heat the solid propellant to the surface temperature.**

## Nomenclature

$a$ = two-flux absorption coefficient
$a_{1\text{-}5}$ = polynomial coefficients for $C_p$ and $H$
$B$ = two-flux back-scatter fraction
$C_d$ = aluminum droplet drag coefficient
$C_p$ = constant pressure specific heat (mass basis)
$C_s$ = specific heat of solid propellant (mass basis)
$c$ = constant in linear regression rate law
$D$ = particle diameter
$fm_i$ = mass fraction of species or mixture $i$
$fv_i$ = volume fraction of species or mixture $i$
$H_i$ = enthalpy (molar basis) of species $i$
$I_{+/-}$ = total radiant intensity (forward/backward)
$k$ = two-flux emission coefficient and proportionality constant in Al burn rate equation
$M_i$ = molecular weight of species or mixture $i$ or generalized chemical species symbol
$m'''_i$ = mass production rate of species $i$ through chemical reaction
$n'''_i$ = molar production rate of species $i$ through chemical reaction
$P$ = pressure
$Q$ = molar enthalpy of combustion
$q_{+/-}$ = total radiant heat flux (forward/backward)
$R$ = molar specific (universal) gas constant
$R_i$ = mass specific gas constant
$r$ = propellant linear regression rate
$s$ = two-flux scattering coefficient
$T$ = temperature
$t$ = time (combustion-flow model) or optical depth (radiation model)
$U$ = velocity
$w$ = single-scatter albedo
$x$ = spatial coordinate normal to and away from propellant surface
$y_i$ = mole fraction of species or mixture $i$
$\alpha$ = absorptivity
$\epsilon$ = emissivity or effective emission coefficient (droplet system)
$\nu'_i, \nu''_i$ = stoichiometric coefficients of reactants and products
$\rho_i$ = density of species or mixture $i$ or reflectivity
$\Sigma$ = summation over $i$ or $j$
$\mu$ = dynamic viscosity

*Subscripts*

AP = ammonium perchlorate
*al* = aluminum droplet (including flame envelope)
B = binder
*b* = blackbody
*bp* = boiling point
*g* = mixture of gaseous species
*go* = mixture of gaseous species and equilibrated aluminum oxide particles
*i* = chemical species or mixture of species
*l* = liquid
*mp* = melting point
*o, ox* = aluminum oxide or initial value
*s* = solid propellant or surface of aluminum droplet
*sp* = surface of solid propellant
*x* = mixture quantity

## Introduction

RADIATIVE heat feedback is often ignored in aluminized composite propellant combustion studies in spite of potentially significant levels of radiant flux produced by condensed Al and $Al_2O_3$ particles. One reason is that studies comparing the burn rates of aluminized and nonaluminized propellants have been inconclusive.[1] Sometimes aluminum enhances the burn rate and sometimes the opposite result is obtained. The percent change in the magnitude of the burn rate in either case is usually small. This behavior is puzzling in light of evidence that external radiation usually increases the burn rate of nonmetallized propellants significantly.[2,3]

The question of whether or not radiative heat feedback is important is complicated by the fact that addition of aluminum changes several properties of the propellant and flame simultaneously (in addition to increasing the radiant heat flux). The thermal conductivity of the propellant is increased by adding aluminum, which tends to increase the burn rate. However, spectrally selective in-depth absorption of the radiant energy by opaque aluminum tends to decrease the burn rate.[4] The overall stoichiometry is often changed by aluminum addition, which could lead to either an increase or a decrease in the burn rate. Also, the replacement of a rate-controlling oxidizer particle size often occurs when aluminum is added. For example, replacing fine ammonium perchlorate (AP) with aluminum usually decreases the burn rate.

Received May 18, 1987; revision received Sept. 23, 1987. 

*Assistant Professor, Department of Mechanical and Industrial Engineering. Member AIAA.

†Graduate Research Assistant, Department of Mechanical and Industrial Engineering.

From these few considerations it can be seen that generalizations about the role of aluminum are still difficult to make. Further systematic study is needed, and one question that needs to be answered is whether the level of radiant flux is sufficient to warrant inclusion in future mechanistic studies or whether it can be neglected. This study tries to answer that question by developing a realistic yet relatively simple model of the flow and combustion of aluminum and the associated thermal radiative transport near the surface of a burning aluminized solid propellant.

## Scope of the Combustion-Radiation Model

The objective of this effort is to predict the radiative heat feedback to a burning composite propellant. This is not intended to be an aluminum combustion efficiency model per se, although it includes many of the same features, such as Al droplet burn rate and two-phase flow considerations. Therefore, not included in this work are Al droplet size distribution effects and two-dimensional flow considerations, both of which are vital to combustion efficiency predictions but of minimal importance to predicting radiative feedback. A recent example of a detailed combustion efficiency model, which is similar in many aspects to this work (but neglects radiation), is that of Larson.[5]

The present model encompasses the region of space several centimeters thick adjacent to the surface of a burning AP composite propellant (Fig. 1). The origin of the $x$ coordinate is at the surface of the burning propellant, which is stationary. The propellant is assumed to move upward at the linear regression rate $r$. The region above the propellant is occupied by combustion gas products of the AP/binder reaction, molten, burning aluminum droplets $Al_{(l)}$, and molten smoke oxide product $Al_2O_{3(l)}$. The AP/binder reaction is assumed to reach equilibrium at the surface of the propellant. The molten aluminum agglomerates are then dragged away from the surface by the hot, high-velocity gaseous species. As the flow proceeds in the positive $x$ direction away from the surface, the Al droplets are accelerated by the flow and, at the same time, reaction with the oxidizing species ($H_2O$, $CO_2$, O, OH, and $O_2$) in the AP/binder products occurs. This results in a decrease in the Al droplet size as the Al is consumed and an increase in the $Al_2O_3$ concentration as the flow moves away from the surface. Eventually the Al is totally reacted and the mixture reaches the final equilibrium composition of the AP/Al/binder flame.

Two phases are considered to be present, a gas phase and a particle phase. (The word "phase" is used broadly here to mean species that have common fluid dynamic and thermodynamic properties, in this case velocity and temperature, as opposed to strictly gas, solid, and liquid.) The gas phase is composed of all the gaseous species as well as the condensed $Al_2O_3$ particles, which have been swept away from the luminous flame envelope surrounding the burning aluminum droplets. These oxide particles and gas are assumed to be in thermal equilibrium at temperature $T_g$ and to have the same velocity $U_g$. The particle phase consists of the burning Al droplets (with temperature $T_{al}$ and velocity $U_{al}$) and the luminous, oxide-laden flame envelope surrounding the droplets.

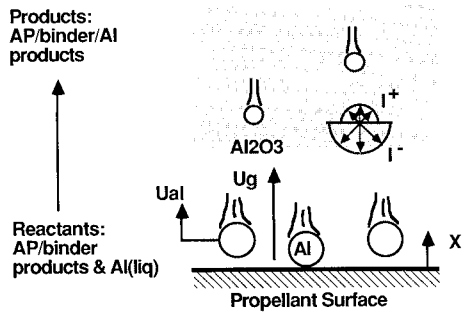


Fig. 1 1-D, 2-phase aluminum flow/combustion-radiation model.

The entire combustion-flow-radiation model is actually composed of two separate models, a combustion-flow model and a radiation model. This separate treatment is made possible by assuming that radiation has negligible influence on energy transport in the gas phase, thus decoupling the energy and radiative transfer equations. The combustion-flow model is first solved to obtain the flowfield and thermodynamic properties. These results are then used in the radiative transfer model to solve for the intensity $I^+$ and $I^-$ using the two-flux model. The quantity of primary interest is the radiant flux $q^-(x=0)=\pi I^-(x=0)$ incident on the propellant surface, assuming reflection and emission by the propellant to be negligible.

Input parameters for the model correspond to those of a typical aluminized AP composite propellant, with 70% AP, 16% Al, and 14% PBAN binder (by mass). Calculations are made at two pressures, 3.44 MPa (500 psia) and 6.87 MPa (1000 psia), covering the most important operating range experienced by most solid rocket motors.

## Aluminum Combustion-Flow Model

The combustion and flow model consists of solving the coupled momentum, energy, mass, and burn rate equations (Table 1). The unknowns are the particle velocity $U_{al}$, gas velocity $U_g$, gas temperature $T_g$, aluminum particle diameter $D_{al}$, and species volume fractions $fv_i$ or mole fractions $y_i$.

**Table 1 Aluminum combustion-flow model**

| Equations | Unknowns |
|---|---|
| Al particle momentum | $U_{al}$ |
| Gas momentum | $U_g$ |
| Energy | $T_g$ |
| Al burn rate | $D_{al}$ |
| Species conservation | $fv_i$ or $y_i$ |

**Table 2 Governing equations (combustion-flow model)**

Al particle momentum

$$\rho_{al(l)} U_{al}\, dU_{al}/dx = 3\rho_g (U_g - U_{al})|U_g - U_{al}|C_d/4D_{al}$$

Gas momentum

$$\rho_{go} fv_{go} U_g\, dU_g/dx = (U_g - U_{al})\, m'''_{al(l)} - 3\rho_g fv_{al(l)} \cdot (U_g - U_{al})|U_g - U_{al}|C_d/4D_{al}$$

Gas energy

$$\rho_{go} fv_{go} C_{pgo} U_g\, dT_g/dx = n'''_{al(l)} Q[T_g, T_{al(l)}]$$

Al energy

$$T_{al} = T_{bp} = 393.3\ \ln [P(Pa)] - 2273$$

Al burn rate

$$D_{al}/D_{oal} = (1 - kt/D_{oal}^{1.8})^{1/1.8}\ \text{(Hermsen)}$$

Species conservation

$$d(\rho_i fv_i U_i)/dx = m'''_i$$

**Table 3 Supporting equations (combustion-flow model)**

Drag coefficient

$$C_d = 24/Re \ (Re < 0.34)$$

$$C_d = 0.48 + 28\ Re^{-0.85} \ (0.34 < Re < 10^5)$$

$$Re = |U_g - U_{al}| D_{al} \rho_g / \mu_g$$

Aluminum production

$$m'''_{al(l)} = -1.667 \rho_{al(l)} f v_{al(l)} k / (D_{oal}^{1.8} - kt) \text{ (Hermsen)}$$

$$k = 8.3314 \times 10^{-5} R_k A_k^{0.9} P(\text{psi})^{0.27} \ (\text{cm}^{1.8}/\text{s})$$

$$A_k = 100\ \Sigma y_i / y_{go} \quad i = \text{H}_2\text{O},\ \text{CO}_2,\ \text{OH},\ \text{O},\ \text{O}_2$$

$$R_k = 2.70$$

$$m'''_i = M_i n'''_i$$

$$n'''_i = (\nu'_i - \nu''_i) n'''_{al(l)}$$

Reaction equation

$$\Sigma \nu'_i M_i + Al_{(l)} \rightarrow \Sigma \nu''_i M_i$$

Enthalpy of combustion

$$Q[T_g, T_{al(l)}] = \Sigma(\nu''_i - \nu'_i) H_i$$

$$H_i/RT_i = a_{1i} + a_{2i} T_i/2 + a_{3i} T_i^2/3 + a_{4i} T_i^3/4 + a_{5i} T_i^4/5 + a_{6i}/T_i$$

Specific heat

$$C_{pi}/R_i = a_{1i} + a_{2i} T_i + a_{3i} T_i^2 + a_{4i} T_i^3 + a_{5i} T_i^4$$

Mixture relations

$$\rho_x = \Sigma f v_i \rho_i / \Sigma f v_i$$

$$f v_i = f m_i \rho_x / \rho_i = y_i \rho_x M_i / (\rho_i M_x)$$

$$M_x = \Sigma y_i M_i / \Sigma y_i$$

$$C_{px} = \Sigma f v_i \rho_i C_{pi} / \Sigma f v_i \rho_i$$

Equation of state

$$\rho_g = P M_g / R T_g$$

Al particle kinematics

$$U_{al} = \text{d}x/\text{d}t$$

### Governing Equations

The governing equations for the combustion-flow model are given in Table 2. The particle momentum equation accounts for acceleration of the aluminum droplets due to the drag force of the gas phase. The gas momentum equation balances the gas acceleration (negative) with the drag force exerted by the aluminum droplets and the momentum required to accelerate the oxide and gas products from the aluminum particle velocity $U_{al}$ to the gas velocity $U_g$. In both momentum equations, pressure and buoyancy forces are neglected. In the gas energy equation, the convective sensible enthalpy rise of the gas oxide mixture is equal to the chemical energy release due to combustion. Both conductive and radiative heat transport have been neglected. Aluminum energy is represented by the assumption that the droplets are isothermal at the metal boiling point. In the species conservation equation, the increase of mass of species $i$ is equal to the volumetric mass production rate of that species through chemical reaction with diffusion mass transport being neglected. The aluminum burn rate is modeled with a "$D^2$-law" using Hermsen's data.[6-8]

### Supporting Equations

Supporting equations for the combustion-flow model are listed in Table 3. These include the aluminum particle drag coefficient $C_d$, the volumetric mass ($m'''_i$) and molar ($n'''_i$) species production terms, the chemical reaction equation, the molar enthalpy of combustion $Q$ ($T_g$, $T_{al}$), the species enthalpies $H_i$ (mass basis) and specific heats $C_{pi}$ (molar basis), the mixture relations, the ideal gas equation of state, and the aluminum particle kinematic equation. Drag on the burning aluminum particles is modeled as drag over a sphere. The volumetric species production terms are generated from reaction stoichiometry and Hermsen's aluminum burn rate model. The thermodynamic properties $H_i$ and $C_{pi}$ are obtained from the widely used NASA polynomial curve-fits of McBride and Gordon.[8-10] The mixture relationships express mixture density, molecular weight, and specific heat in terms of the corresponding individual constituent quantities.

In this work, any of three equivalent concentration parameters may be used to indicate chemical composition: volume fraction, mass fraction, or mole fraction. Mole fractions are used most commonly in connection with chemical equilibrium calculations. Volume fractions are the easiest to use in deriving the governing conservation equations and also appear in the particulate radiative transfer relations. And mass fractions are commonly used for specifying propellant composition. Therefore, all three descriptors are used in various places in this work and an equation is supplied in the mixture relations for converting between any two of the three. It should also be noted that the use of volume fractions implies adoption of the Amagat model of ideal gas mixtures and, therefore, all species are envisioned as having the same pressure but occupying individual volumes (i.e., partial pressure has no meaning).

### Aluminum Burn Rate Modification

One term in the Hermsen burn rate law deserves special discussion. In the aluminum production terms of Table 3, the term $A_k$ describes the influence of the ambient chemical composition on Al burn rate. This term is defined in Ref. 8 as the sum of the mole percent of oxidizing species in the ambient environment. High values of $A_k$ corresponding to high oxidizer concentrations result in higher burning rates and vice versa. Since the empirical constants in the model are obtained from laboratory experiments where the radiation environment and velocity lag are different than the motor environment, an empirical factor $R_k$ has also been added to compensate for these two effects.

The problem unique to this study is that if the prescribed definition of $A_k$ is used, the predicted Al burn rates near the surface will probably be too low. This is because the empirical constants have been obtained assuming constant oxidizer mole fractions. In a rocket motor environment, the highest mole fraction of aluminum, when calculated in a "batch" sense (i.e., neglecting velocity slip of aluminum droplets), is about 16%. However, near the surface of the propellant, the velocity slip between aluminum droplets and oxidizing gases and the high density of aluminum relative to the gaseous species results in mole fractions of aluminum of approximately 97 and 59% at the propellant surface at 3.44 MPa (500 psia) and 6.87 MPa (1000 psia), respectively. If the mole fractions of oxidizing gases are based on the total mixture (with aluminum occupying 59–97% near the surface), the predicted aluminum burn rates will be too low. Therefore, the term $y_{go}$ [moles of gas/oxidizer (gas phase) per mole of total mixture] is included

in the denominator of the $A_k$ expression. This has the effect of putting the oxidizer mole fractions used in $A_k$ on a basis relative to the gas phase rather than the total mixture, more in line with the experiments used to obtain the burn rate data.

**Initial Conditions**

The initial conditions used in solving the governing equations for the combustion-flow model are listed in Table 4. The initial aluminum volume fraction is obtained from conservation of aluminum across the propellant surface, assuming that there is no reaction between aluminum and the surrounding AP/binder and that the initial aluminum velocity at the moment the droplet ignites and begins to leave the surface is the linear regression rate of the propellant. The initial aluminum volume fraction is thus the volume fraction in the propellant modified by a slight change in density of the aluminum upon melting. This treatment does not address the mechanism of aluminum agglomeration. Thus, it does not preclude the possibility of aluminum concentration on the surface prior to agglomeration. It does not predict the agglomerate size either. The initial velocity of aluminum is so small compared with the surrounding gas velocity that it could be taken as zero.

The initial gas velocity is obtained from conservation of mass of the AP/binder matrix across the propellant/gas interface, assuming that the AP/binder reactions reach equilibrium at or very near the surface. As the AP and binder react, the density decreases by a factor of 200–300 (depending on pressure), resulting in an increase of similar magnitude in the gas velocity over the propellant burn rate.

**Table 4 Initial conditions for combustion-flow model**

| | |
|---|---|
| $U_{al} = r$ | $[fv_{al(l)} = fv_{al(s)}\ \rho_{al(s)}/\rho_{al(l)}]$ |
| $U_g = fv_{\mathrm{AP,B}}\ r\rho_{\mathrm{AP,B}}/(\rho_g fv_g)$ | $[fv_g = 1 - fv_{al(l)}]$ |
| $T_g = 2384$ K | |
| $D_{oal} = 1/[1.1248\ r(\mathrm{m/s})]\ fm_{\mathrm{AP}}$ | |
| $y_i = \nu'_i[1 - y_{al(l)}]/\Sigma\nu'_j$ [sum over all $j$ except Al($l$)] | |
| $y_{al(l)} = fm_{al(l)}M_x/M_{al}$ | |
| $M_x = M_g y_g + M_{al}y_{al(l)}$ | |
| $y_g = 1 - y_{al(l)}$ | |
| $M_g = \Sigma\nu'_i M_i/\Sigma\nu'_i$ [sum excludes Al($l$) and $Al_2O_3$] | |
| $fm_{al(l)} = fv_{al(l)}\ \rho_{al(l)}/\rho_x$ | |
| $\rho_x = fv_{al(l)}\rho_{al(l)} + fv_g\rho_g$ | |
| $fv_g = fv_{\mathrm{AP}} + fv_{\mathrm{B}}$ | |
| $\rho_g = \mathrm{P}M_g/\mathrm{RT}_g$ | |
| $fv_{al(l)} = fv_{al(s)}$ | |
| $fv_{al(s)} = fm_{al(s)}\ \rho_s/\rho_{al(s)}$ | |
| $fv_{\mathrm{AP}} = fm_{\mathrm{AP}}\rho_s/\rho_{\mathrm{AP}}$ | |
| $fv_{\mathrm{B}} = fm_{\mathrm{B}}\rho_s/\rho_{\mathrm{B}}$ | |
| $\rho_s = 1/[fm_{al(s)}/\rho_{al(s)} + fm_{\mathrm{AP}}/\rho_{\mathrm{AP}} + fm_{\mathrm{B}}/\rho_{\mathrm{B}}]$ | |

The initial gas temperature is taken as the equilibrium adiabatic flame temperature of the AP/binder reaction at 3.44 MPa (500 psia), 2384 K. Since this is above the melting point of aluminum oxide (2320 K), solid $Al_2O_3$ is never encountered. Also, since energy is required to melt the solid aluminum in the propellant and raise it to its boiling point, an appropriate amount of energy 116 KJ/mole (27,767 cal/mole) is removed from the initial enthalpy of AP in this calculation to account for the energy lost from the AP/binder system. The temperature of 2384 K reflects this modification.

The initial aluminum agglomerate diameter is calculated from a correlation of Nickerson et al.[8] The initial droplet sizes were 145 $\mu$m and 115 $\mu$m at 3.44 and 6.87 MPa (500 and 1,000 psia), respectively.

Determining the mole fractions at the surface is a little more difficult than just taking the equilibrium mole fractions from the AP/binder reaction and adding the proper stoichiometric proportion of aluminum. To do so would neglect the aluminum velocity lag at the surface and grossly underpredict the aluminum mole fraction at the surface. Instead, the starting point for the initial mole fraction determination is the statement of conservation of aluminum across the propellant surface, $fv_{al(l)} = fv_{al(s)}\rho_{al(s)}/\rho_{al(l)}$. The initial volume fraction $fv_{al(s)}$ can be determined from the initial mass fraction of aluminum in the propellant, $fm_{al(s)}$. The volume fraction of liquid aluminum above the surface $fv_{al(l)}$ can then be converted into the mole fraction $y_{al(l)}$ using the mixture relations of Table 3. From $y_{al(l)}$, the initial mole fractions of all the other species can be determined using the mole numbers $\nu'_i$, which are developed from the equilibrium AP/binder flame composition. It should perhaps be noted that the expression for gas molecular weight $M_g$ in Table 4 is used only for the initial calculation, and thereafter the general mixture relation of Table 3 is used. In solving the system of governing equations, the volume fractions were actually converted into mole fractions, and the product of mole fraction times mixture density $y_i\rho_x$ was solved. This quantity could then be summed over all species to obtain the mixture density $\rho_x$, which could be divided into $y_i\rho_x$ to give the mole fractions.

**Numerical Solution of the Governing Equations**

The governing equations were written in finite-difference form and solved numerically on a digital computer. Input data for the AP/binder and AP binder/Al/chemical equilibrium problems were obtained from the ODE module of the Air Force Rocket Propulsion Laboratory solid propellant program (SPP).[8] A step size $\Delta^x$ of 10 $\mu$m was used in the combustion-flow model. The step size was increased to 100 $\mu$m for the radiation model. This increase in step size was found to be necessary to adequately model the radiative influence of the agglomerates on the surface, which were of the order of 100 $\mu$m. The aluminum volume fraction decreased so quickly away from the surface that it was necessary to force the surface value of aluminum volume fraction to extend over a step size of the order of the agglomerate size to correspond to the actual physical situation and thus accurately model the presence of the droplets near the surface.

Since diffusive mass, heat, and momentum transfer effects are neglected in the governing equations, the corresponding second-order derivative terms do not appear. The equations are forward-differenced and solved in an explicit marching scheme. That is, the known values at the first half-node are used to calculate the unknown values at the second full node, and so on.

**Parameters Used in the Combustion-Flow Model**

Other properties and parameters used in the aluminum combustion-flow model are listed in Table 5. The gas viscosity was taken to be constant at the value of the AP/binder flame products (3.44 MPa). Aluminum and oxide densities were also assumed to be independent of temperature.[11] Burn rate and propellant composition data for a typical AP composite

propellant were used in the calculations. The reactant and product stoichiometric coefficients for the 27 chemical species considered are listed in Table 6. The reactant values $\nu'_i$ were calculated from the equilibrium mole fractions of the AP/binder flame based on one mole of $Al_{(l)}$ (with the input enthalpy of AP reduced to compensate for the aluminum melting and preheating, as noted earlier). The product values $\nu''_i$ were calculated from the equilibrium mole fractions of the AP/Al/binder flame based on zero moles of $Al_{(l)}$ in the products. Reactant mole numbers of aluminum compounds other than $Al_{(l)}$ are set to zero to be consistent with the assumption of no reaction between aluminum and AP below the propellant surface.

## Radiation Model

Previous efforts to model radiative transfer in aluminized rocket motors have pointed out the need for including the effect of scattering by condensed $Al_2O_3$.[12] In this study the two-flux model of radiative transport is used. The surface of the propellant is taken to be a blackbody at zero degrees as indicated by the nonreflecting, nonemitting boundary condition. This condition can be easily modified later by including the actual scattering characteristics of the propellant and treating the problem as radiant interchange between two plane, parallel walls with the appropriate effective absorptivities, emissivities, and reflectivities.

Particulate radiation only is considered (gaseous radiation would be negligible). Participation by both oxide smoke particles in the gas phase and the burning aluminum droplets of the particle phase is considered. The alumina particles are assumed to be spherical and monodisperse (as are the aluminum droplets). The appropriate expressions for the scattering, absorption, and emission coefficients for these assumptions are given in Table 7.

The use of an emission coefficient separate from the absorption coefficient in Table 7 should be noted, since they usually are the same. This distinction is made necessary here by the fact that the burning $Al/Al_2O_3$ droplet systems are not in thermodynamic equilibrium. The properties of these droplets are effective properties representing the complex radiative transfer that actually occurs in the luminous, nonisothermal, oxide-laden flame envelope surrounding the droplet and between the flame envelope and the droplet itself. These effects have been considered elsewhere,[13] and the appropriate results of that study have been incorporated here.

The key finding of Ref. 13 is that the envelope around the burning droplet, although optically thin (thus contributing negligibly to scattering and absorption), is nevertheless a strong source of emission due to the high temperature in the envelope (approximately the oxide boiling point $T_{oxbp}$). The effective emissivity of a burning droplet (based on droplet temperature $T_s$) can be represented by the three-term expression in Table 7 for $\epsilon_{al}$ in which $t_e$ is the optical depth of the flame envelope. The three terms correspond to direct emission (1), envelope emission reflected from the droplet surface (2), and droplet emission (3). From measurements of intensity emitted by burning aluminum droplets at the surface of aluminized AP pressed pellets, it was determined that $\epsilon_{al}$ was the order of 1.0 (Table 8). This estimate is based on the following values: $T_s = 2320$ K, $T_{oxbp} = 4820$ K (6.9 MPa), $t_e\epsilon_{ox} = 0.01$ to 0.02, $\rho_s = 0.9$, and $\epsilon_s = 0.1$. Based on a different assumed droplet temperature $T_s$, $\epsilon_{al}$ would be increased or decreased by the ratio $(T_s/2320)^4$ but the emitted

**Table 5 Parameters used in combustion-flow model**

| | |
|---|---|
| Gas | $\mu_g = 0.744 \times 10^{-4}$ kg/ms |
| Aluminum (liquid) | $\rho_{al(l)} = 2350$ kg/m$^3$ |
| Aluminum oxide (liquid) | $\rho_{ox} = 3690$ kg/m$^3$ |
| Burn rate | $r(\text{m/s}) = cP(\text{Pa})^n$<br>$c = 0.44652 \times 10^{-4}$<br>$n = 0.35$ |

Solid propellant properties

| | | AP/Aℓ/Binder | | AP/Binder | |
|---|---|---|---|---|---|
| Constituent | $\rho$(kg/m$^3$) | $H$(Cal/mole) | $fm$ | $H$(Cal/mole) | $fm$ |
| *Al (s)* | 2700 | 0 | 0.16 | 0 | 0 |
| AP | 1950 | −70,690 | 0.70 | −98,457 | 0.833 |
| Binder | 950 | −15,110 | 0.14 | −15,110 | 0.167 |

**Table 6 Stoichiometric coefficients**

| $M_i$ | $\nu'_i$ | $\nu''_i$ |
|---|---|---|
| $Al_2O_{3(l)}$ | 0 | 0.475 |
| $Al_{(l)}$ | 1 | 0 |
| Al | 0 | $0.560 \times 10^{-3}$ |
| AlCl | 0 | $0.247 \times 10^{-1}$ |
| $AlCl_2$ | 0 | $0.845 \times 10^{-2}$ |
| $AlCl_3$ | 0 | $0.750 \times 10^{-3}$ |
| AlH | 0 | $0.800 \times 10^{-4}$ |
| AlO | 0 | $0.114 \times 10^{-2}$ |
| AlOCl | 0 | $0.947 \times 10^{-2}$ |
| AlOH | 0 | $0.225 \times 10^{-2}$ |
| $AlO_2$ | 0 | $0.210 \times 10^{-3}$ |
| $AlO_2H$ | 0 | $0.378 \times 10^{-2}$ |
| $Al_2O$ | 0 | $0.180 \times 10^{-3}$ |
| CO | $0.104 \times 10^{1}$ | $0.148 \times 10^{1}$ |
| $CO_2$ | 0.545 | 0.106 |
| Cl | $0.530 \times 10^{-2}$ | $0.829 \times 10^{-1}$ |
| H | $0.488 \times 10^{-2}$ | 0.235 |
| HCl | 0.999 | 0.870 |
| HCN | 0 | $0.300 \times 10^{-4}$ |
| $H_2$ | 0.658 | $0.164 \times 10^{1}$ |
| $H_2O$ | $0.198 \times 10^{1}$ | 0.915 |
| N | 0 | $0.400 \times 10^{-4}$ |
| NO | $0.140 \times 10^{-3}$ | $0.433 \times 10^{-2}$ |
| $N_2$ | 0.528 | 0.527 |
| O | $0.100 \times 10^{-4}$ | $0.484 \times 10^{-2}$ |
| OH | $0.262 \times 10^{-2}$ | $0.566 \times 10^{-1}$ |
| $O_2$ | $0.200 \times 10^{-4}$ | $0.107 \times 10^{-2}$ |

**Table 7 Governing equations (radiation model)**

Two-flux model

$$dI^+/dx = -(a+s)I^+ + sI^- + k_{al}I_b(T_s) + k_{ox}I_b(T_g)$$
$$-dI^-/dx = -(a+s)I^- + sI^+ + k_{al}I_b(T_s) + k_{ox}I_b(T_g)$$

$$I^+(x=0) = 0$$
$$dI^+/dx(x \to \infty) = 0$$

Two-flux coefficients

$$a = a_{al} + a_{ox}$$
$$s = s_{al} + s_{ox}$$

$$a_i = 3fv_i\,\alpha_i/D_i;\ i = al,\ ox$$
$$s_i = 3fv_i\,\rho_i\,B_i/D_i$$
$$k_i = 3fv_i\,\epsilon_i/D_i$$

$$\epsilon_{al}(T_s) = \underbrace{2t_e\epsilon_{ox}I_b(T_{oxbp})/I_b(T_s)}_{(1)} + \underbrace{2t_e\epsilon_{ox}\rho_s I_b(T_{oxbp})/I_b(T_s)}_{(2)} + \underbrace{\epsilon_s}_{(3)}{}^{a}$$

[a]Ref. 13.

**Table 8 Parameters used in radiation model**

| | $\alpha$ | $\rho$ | $\epsilon$ | B |
|---|---|---|---|---|
| Burning aluminum droplets (including flame envelope) | 0.10 | 0.90 | 1.0[a] | 0.50 |
| Aluminum oxide | 0.45 | 0.55 | 0.45 | 0.30 |

[a]Based on 2320 K.

intensity would be the same. Thus, the use of 2320 K for the droplet temperature in the radiation calculation is arbitrary and is not inconsistent with the use of the metal boiling point in the thermodynamic analysis. Substituting the given values into the relation for $\epsilon_{al}$ in Table 7 shows that emission by the envelope (terms 1 and 2) contributes 90% of total droplet emission, in spite of the low optical thickness of the envelope. Thus, the envelope represents a significant portion of the droplet emission.

The optical constants and size distribution of rocket $Al_2O_3$ have been studied by many investigators.[14-28] Although extinction efficiency, albedo, and scattering asymmetry are strong functions of particle size and wavelength, for total radiant heat flux predictions, the concept of an effective gray monodispersion is valid provided the correct size, effective albedo, and scattering asymmetry are used.[18] In this study an effective size of 0.3 $\mu$m, an effective albedo of 0.55 (emissivity of 0.45), and a two-flux back scatter of 0.3 were used. These values, obtained from Ref. 17, are in line with results of other investigators.[15,16] Reference 15 reports measured size distributions for rocket exhaust particles with most probable sizes of 0.2 $\mu$m. Calculations comparing actual polydispersion properties with effective monodispersions for typical size distribution functions indicate that the effective monodisperse diameter is usually about 1.5 times the most probable diameter in this size parameter range.[18] Thus, an effective diameter of 0.3 $\mu$m seems quite reasonable.

The effective albedo of molten alumina is highly uncertain at this time. Part of the reason is that it is very sensitive to the level of contaminants present (e.g., carbon, aluminum, ferric oxide, etc.),[19,20,26] and part of the reason is that it is very sensitive to the combination of optical constants and size distribution assumed.[15] Where incompatible sets of data for optical constants and size distribution are mixed, arbitrary and erroneous effective albedos are obtained. As a result, albedos for molten alumina have been reported ranging from near zero[21] to as high as 0.925.[12] Other recent studies favor values in the 0.7-0.8 range.[15] Obviously this issue needs further investigation. For the purposes of this study we have chosen to use the effective albedo of 0.55 from Ref. 17.

## Results

The combustion-flow model results at 3.44 MPa (500 psia) and 6.87 MPa (1000 psia) are presented in Figs. 2-6, with radiation results in Figs. 7-9. Figure 2 shows the decrease in aluminum diameter above the propellant with burnout occurring 6 cm (3.44 MPa) and 2 cm (6.87 MPa) from the surface. The initial rapid decrease in the aluminum diameter with distance is due to the velocity slip near the surface, which can be seen in Fig. 3. Figure 4 shows that the gas temperature rises rapidly near the surface and eventually approaches the adiabatic AP/binder/Al flame temperature of 3374 K.

The mole fractions of the major fuel ($Al_{(l)}$) product ($Al_2O_3$) and oxidizer species ($H_2O$) are plotted in Fig. 5 for 6.87 MPa. The oxide mole fraction increases due to progressive aluminum combustion, and the aluminum fraction decreases as expected. The very rapid decrease in aluminum fraction in the first few millimeters is due mostly to acceleration of the aluminum droplets. The $H_2O$ profile (which is typical of the other oxidizing species) increases initially due to aluminum

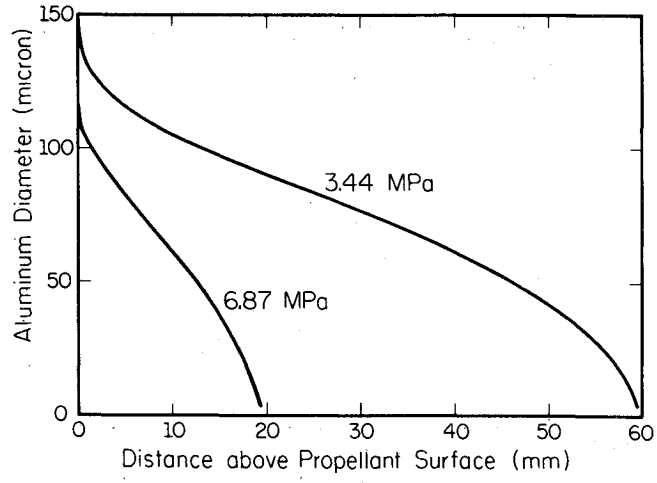


**Fig. 2 Aluminum diameter.**

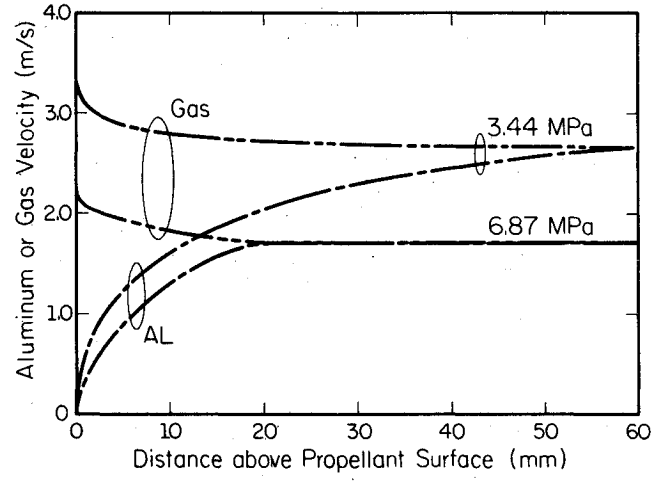


**Fig. 3 Aluminum and gas velocity.**

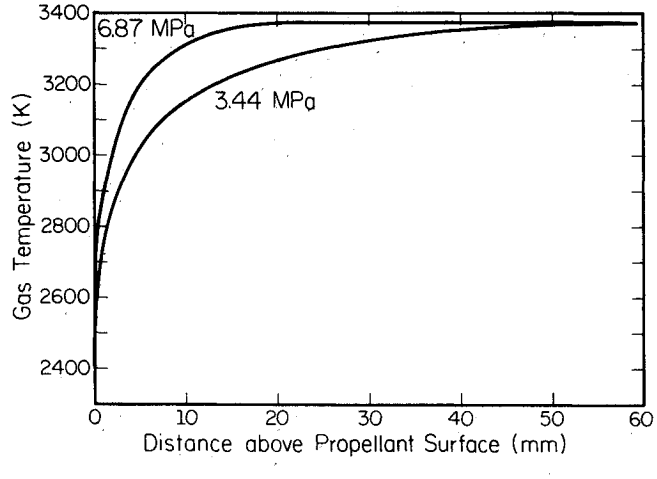


**Fig. 4 Gas temperature.**

acceleration and then decreases as it is consumed by combustion. Similar species profiles are obtained for the 3.44-MPa case with the variations stretched over 60 mm instead of 20 mm.

Volume fractions of alumina and aluminum are also plotted in Fig. 6 because of the important role they play in the radiative properties. The alumina volume fraction reaches $10^{-4}$ within 1 mm of the surface at 3.44 MPa, while the aluminum drops from $10^{-1}$ to $10^{-3}$ in the same distance.

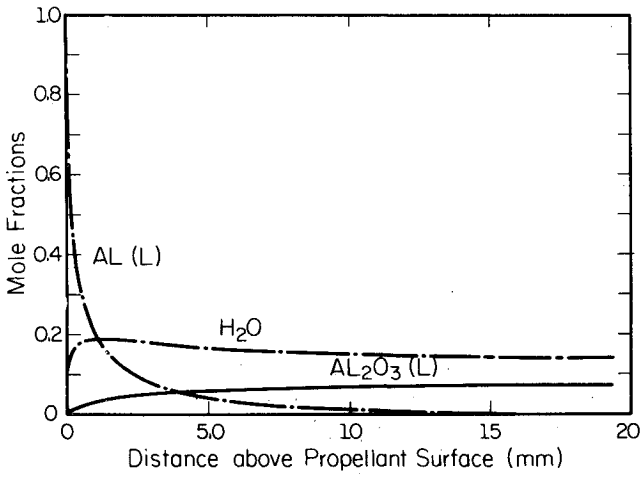


**Fig. 5 Major constituent mole fractions (6.87 MPa).**

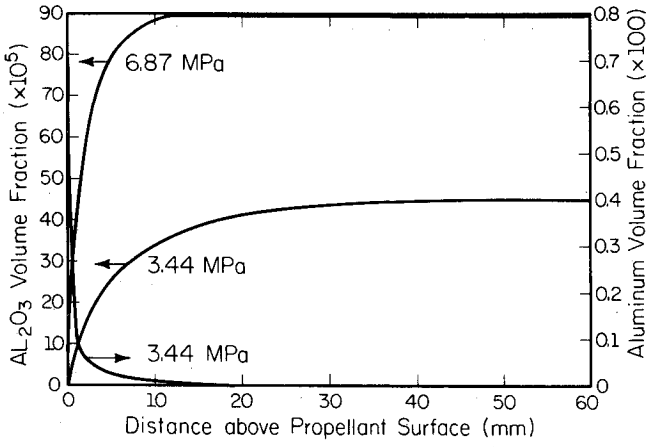


**Fig. 6 $Al_2O_3$ and Al volume fractions.**

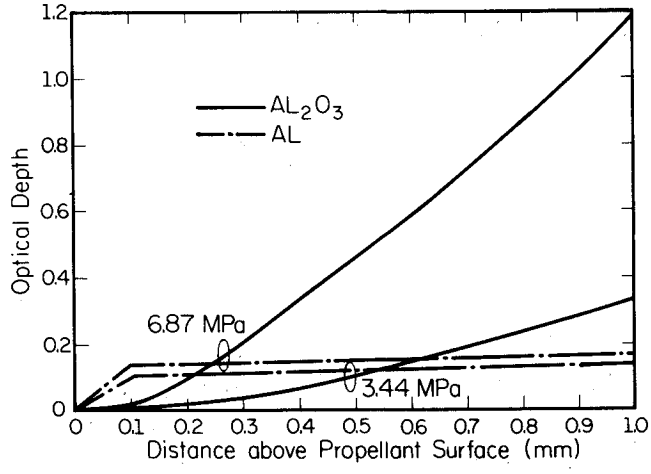


**Fig. 7 Optical depth of Al and $Al_2O_3$.**

The optical depth normal to the propellant surface due to alumina and that due to aluminum are plotted in Fig. 7. Within about 300–600 $\mu$m of the surface, the two optical depths are of comparable magnitude. Beyond that point, the oxide begins to dominate, and the medium eventually becomes optically thick due to oxide.

The radiant fluxes ($q = \pi I$) are plotted in Fig. 8. Near the surface the forward flux (away from the surface) is very small due to the nonreflecting, nonemitting boundary condition. The backward flux (toward the propellant) at $x = 0$ represents the flux that would be incident on the propellant surface and for $\epsilon_{al} = 1$ has a magnitude of 290 W/cm$^2$ (3.44 MPa) and 330

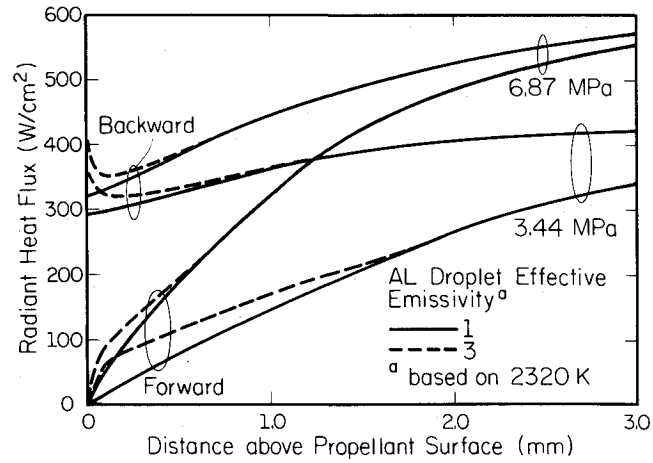


**Fig. 8 Forward and backward radiant heat flux.**

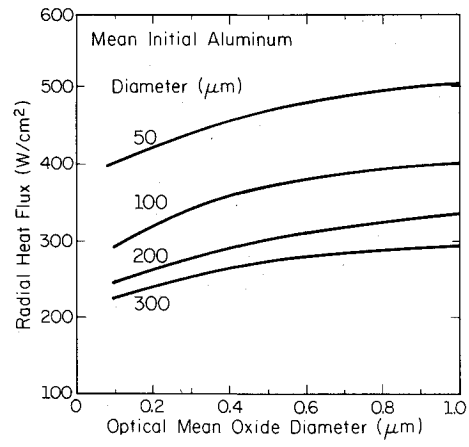


**Fig. 9 Effect of Al and $Al_2O_3$ size on radiant heat feedback (6.87 MPa, $\epsilon_{al} = 1$).**

W/cm$^2$ (6/87 MPa). Because of the uncertainty that still remains in the actual value of the effective emissivity of burning aluminum droplets, the radiant flux is also presented for an assumed vlaue of $\epsilon_{al} = 3$ (based on 2320 K). This value is felt to be near the upper limit and is based on extrapolation from reported brightness and color temperatures of aluminum photo flash lamps.[22] It may be argued that since the value of $\epsilon_{al} = 1$ was determined from measurements of burning droplets in pure AP flames, a higher value is appropriate for propellant flames due to the higher temperature of the gas surrounding the droplets (2300–2400 K compared with 1200–1400 K for AP). This difference in gas temperature could make a significant difference in the intensity emitted by the condensed $Al_2O_3$ in the flame envelope. The results in Fig. 8 for $\epsilon_{al} = 3$ show that the burning aluminum droplets contribute significantly to the radiant heat feedback to the propellant surface by increasing the flux to 360 W/cm$^2$ (3.44 MPa) and 400 W/cm$^2$ (6.87 MPa). Since the flame envelope is at such a high temperature and is such a significant source of emission from the droplets, the spectral distribution of the flux back to the propellant would be represented by blackbody radiation at 4000–4800 K, while the magnitude of the flux would correspond to a blackbody at 2700–2900 K.

To investigate the effect of the assumed aluminum and oxide particle sizes on the radiant flux, additional calculations were performed varying these sizes, and the results are presented in Fig. 9. It can be seen that smaller aluminum droplets, which would tend to burn out closer to the propellant surface, would result in more radiant heat feedback. Smaller oxide particles, on the other hand, would tend to decrease the radiant feedback due to an increase in optical depth in the relatively cold region near the propellant surface.

**Table 9 Heat flux to propellant surface (W/cm²)**

| Incident radiant heat flux (% of total) | | |
|---|---|---|
| Heat flux (W/cm²) | 3.44 MPa | 6.87 MPa |
| $q^a$ | 1240 | 1560 |
| $q$ rad ($\epsilon_{al} = 1$) | 290 (23%) | 330 (21%) |
| $q$ rad ($\epsilon_{al} = 3$) | 360 (29%) | 400 (26%) |

$$q^a = \rho_{sp} r C_{sp} (T_{sp} - T_o)$$

$\rho_{sp} = 1.77$ g/cm³; $C_{sp} = 1.4$ J/gK
$T_{sp} = 875$ K; $T_o = 300$ K

[a]Required to heat propellant to surface temperature $T_{sp}$.

## Comparison with Total Heat Feedback Requirement

The radiant heat feedback predicted by this model is compared in Table 9 with an estimate of the total energy flux required to raise the initial, cold solid propellant to an average surface temperature of 875 K. Although complex details of the heat transfer at the surface are ignored by taking the energy balance below the propellant surface, this comparison is probably still valid because most of the radiant energy would be transmitted past the complex surface zone and absorbed or scattered in depth4 below the surface. The total energy flux requirement is estimated as 1240 and 1560 W/cm² at 3.44 and 6.87 MPa, respectively. For a burning droplet emissivity of $\epsilon_{al} = 1$, the fraction of radiant contribution to the total heat feedback is estimated as 23% at 3.44 MPa and 21% at 6.87 MPa. These percentages increase to 29% and 26%, respectively, for $\epsilon_{al} = 3$, based on 2320 K.

It is also interesting to consider radiative effects connected with the spectral distribution of the radiation heat feedback. As noted earlier, although the flux levels correspond to blackbody radiation at 2700–2900 K, the spectral distribution is probably closer to that of a blackbody at 4000–4800 K, depending on pressure. Assuming 4000 K, half of the radiant energy would be below 1 $\mu$m wavelength, which is the approximate cutoff wavelength for absorption for many of the transition metal oxides that have demonstrated significant catalytic behavior in composite propellants (e.g., $Fe_2O_3$, $Cr_2O_3$, $Cu_2O$, CuO, copper chromite, etc.), This suggests the possibility of a selective absorption/emission mechanism acting instead of or in addition to the chemical catalytic mechanism.

## Conclusions

Development of a model for combustion, flow, and radiation by aluminum and aluminum oxide near the surface of a burning solid propellant has led to the conclusion that the level of radiant flux back to the propellant surface is 300–400 W/cm2, which represents about 20% of the total energy flux required to heat the solid propellant to the surface temperature. This radiant contribution may be partially responsible for the pressure decoupling influence aluminum addition seems to have on oscillatory solid propellant combustion. The radiation contribution should be considered more carefully in future mechanistic combustion studies.

## Acknowledgments

Support for this work from the National Science Foundation (CBT86-96162), Morton Thiokol Inc./Wasatch Division, and the Office of Naval Research is gratefully acknowledged.

## References

[1]Price, E. W., "Combustion of Metallized Propellants," *Fundamentals of Solid Propellant Combustion, Progress in Astronautics and Aeronautics Series*, Vol. 90, edited by K. K. Kuo and M. Summerfield, AIAA, New York, 1984, p. 502.

[2]Caveny, L. H., Ohlemiller, T. J., and Summerfield, M., "Influence of Thermal Radiation on Solid Propellant Burning Rate," *AIAA Journal*, Vol. 13, Feb. 1975, p. 202–205.

[3]Ibiricu, M M. and Willimas, F. A., "Influence of Externally Applied Thermal Radiation on the Burning Rates of Homogeneous Solid Propellants," *Combustion and Flame*, Vol. 24, 1975, pp. 185–198.

[4]Brewster, M Q. and Patel, R. S., "Selective Radiative Preheating of Aluminum in Composite Solid Propellant Combustion," *Journal of Heat Transfer*, Vol. 109, No. 1, 1987, pp. 179–184.

[5]Larson, R. S., "Prediction of Aluminum Combustion Efficiency in Solid Propellant Rocket Motors," *AIAA Journal*, Vol. 25, Jan. 1987, pp. 92–91.

[6]Hermsen, R. W., "Improved Technical Elements for SSP: Combustion Efficiency Models," CPIA 321, 7180, pp. 53–60.

[7]Salita, M., "Physical Model and Numerical Correlations to Predict Combustion Inefficiency in Solid Rocket Motors," Morton-Thiokol/Wasatch Div., UT, IOM 2814-80-M154, Dec. 1980.

[8]Nickerson, G. R., Coats, D. E., Hermsen, R. W., and Lamberty, J. T., "A Computer Program for the Prediction of Solid Propellant Rocket Motor Performance (SPP)," Vols. 1–5, AFRPL TR-83-036, Sept. 1984.

[9]Gordon, S. and McBride, B. J., "Computer Program for Calculation of Complex Equilibrium Compositions, Rocket Performance, Incident and Reflected Shocks, and Chapman-Jouget Detonations," NASA SP 273, 1971.

[10]McBride, B. J. and Gordon, S., "Fortran IV Program for Calculation of Thermodynamic Data," NASA TN-D-4097, 1967.

[11]Micheli, P. L. and Schmidt, W. G., "Behavior of Aluminum in Solid Rocket Motors," AFRPL TR-77-29, Vol. 1, 1977.

[12]Pearce, B. E., "Radiative Heat Transfer within a Solid Propellant Rocket Motor," *Journal of Spacecraft and Rockets*, Vol. 15, March–April, 1978, pp. 125–128.

[13]Brewster, M. Q. and Taylor, D. M., "Radiative Properties of Burning Aluminum Droplets," presented as Paper WSS/CI 87-13 at Western States Section/Combustion Institute Meeting, Provo, UT, April 6–7, 1987; also *Combustion and Flame* (submitted for publication).

[14]Gal, G. and Kirch, H., "Particulate Optical Properties in Rocket Plumes," AFRPL-TR-73-99, Nov. 1973, pp. 28–29.

[15]Konopka, W. L., Reed, R. A., and Calia, V. S., "Measurements of Infrared Optical Properties of $Al_2O_3$ Rocket Particles," *Progress in Astronautics and Aeronautics*, Vol. 91, 1984, pp. 180–197.

[16]Driscoll, J. E., Nicholls, J. A., Patel, V., Shahidi, B. K., and Liu, T. C., "Aluminum Combustion at 40 Atmospheres Using a Reflected Shock Wave," *AIAA Journal*, Vol. 24, May 1986, pp. 856–858.

[17]Brewster, M. Q. and Parry, D. L., "In-Situ Measurements of Alumina Particle Size and Optical Constants," AIAA Paper 87-1582, June 1987.

[18]Hansen, J. E. and Travis, L. D., "Light Scattering in Planetary Atmospheres," *Space Science Reviews*, Vol. 16, 1974, pp. 527–610.

[19]Pluchino, A. B. and Masturzo, D. E., "Emissivity of $Al_2O_3$ Particles in a Rocket Plume," *AIAA Journal*, Vol. 19, Sept. 1981, pp. 1234–1237.

[20]Rieger, T. J., "On the Emissivity of Alumina/Aluminum Composite Particles," *Journal of Spacecraft and Rockets*, Vol. 16, Nov.–Dec. 1979, pp. 438–439.

[21]Glassman, I., "Combustion of Metals Physical Considerations," *Progress in Astronautics and Rocketry*, Vol. 1, 1960, pp. 253–257.

[22]Rautenberg, T. H. Jr. and Johnson, P. D., "Light Production in Aluminum-Oxygen Reaction," *Journal of the Optical Society of America*, Vol. 50, No. 6, June 1960, pp. 602–606.

[23]Drew, C. M., Gordon, A. S., and Knipe, R. H., "Study of Quenched Aluminum Particle Combustion," *Progress in Astronautics and Aeronautics*, Vol. 15, 1964, pp. 17–39.

[24]Carlson, D. J., "Emittance of Condensed Oxides in Solid Propellant Combustion Products," Tenth Symposium (International) on Combustion, The Combustion Institute, 1965, pp. 1413–1424.

[25]Adams, J. M., "A Determination of the Emissive Properties of a Cloud of Molten Alumina Particles," *Journal of Quantitative Spectroscopy and Radiative Transfer*, Vol. 7, 1967, pp. 273–277.

[26]Dobbins, R. A. and Strand, L. D., "A Comparison of Two Methods of Measuring Particle Size of $Al_2O_3$ Produced by a Small Rocket Motor," *AIAA Journal*, Vol. 8, No. 9, Sept. 1970, pp. 1544–1550.

[27]Mularz, E. J. and Yuen, M. C., "An Experimental Investigation of Radiative Properties of Aluminum Oxide Properties," *Journal of Quantitative Spectroscopy and Radiative Transfer*, Vol. 12, 1972, pp. 1553–1568.

[28]Orguc, S., Pruitt, T. E., Edwards, T. D., Youngborg, E. D., Powers, J. P., and Netzer, D. W., "Measurement of Particulate Size in Solid Propellant Rocket Motors," *Proceedings of 1987 JANNAF Combustion Meeting* (to be published) CPIA Publications.